CROSS-SECTIONAL MEASURING OF OPTICAL BEAM

Tomas DAVID[1], *Jan LATAL*[1], *Frantisek HANACEK*[1], *Petr KOUDELKA*[1], *Jan VITASEK*[1], *Petr SISKA*[1], *Jan SKAPA*[1], *Vladimir VASINEK*[1]

[1]Department of Telecommunications, Faculty of Electrical Engineering and Computer Science, VSB – Technical University of Ostrava, 17. listopadu 15, 708 33 Ostrava, Czech Republic

dav079@vsb.cz, jan.latal@vsb.cz, frantisek.hanacek@vsb.cz, petr.koudelka@vsb.cz, jan.vitasek@vsb.cz, petr.siska@vsb.cz, jan.skapa@vsb.cz, vladimir.vasinek@vsb.cz

Abstract. *This article deals with problematic of measuring of optical beam in free space optics (FSO). The professional FSO link was created between two buildings standing 1,5 kilometers apart from each other. Signal passing through the atmospheric media between optical heads is affected. This happens due to effects in atmospheric media. This article describes creating of the device for measuring the intensity of optical beam in 2D space and its subsequent rendering into 3D graph.*

Keywords

Free space optics, atmospheric media, turbulence, optical beam, measuring.

1. Introduction

The FSO link consists of two optical heads operating in full duplex mode, both as transmitter and receiver (Fig. 1). These optical heads are situated against each other and must be in direct line of sight. Optical head is usually placed on the roof of buildings, but it can also be placed in windows.

Each optical head has an emitting source, in our case it is a laser diode, which provides conversion of signals from electrical to optical domain. After that, the output signal is shaped by optical lens to desired shape. The resulting beam transmitting from head is of Gaussian intensity distribution.

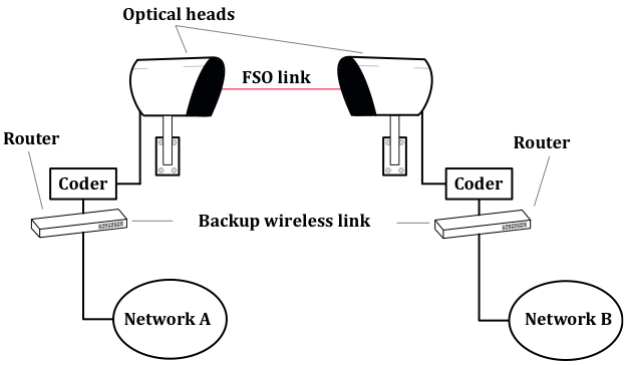

Fig. 1: Scheme of FSO link [1], [12].

2. Gaussian Beam

Intensity distribution of Gaussian beam in the transverse plane corresponds to a circularly symmetric Gaussian function, where the optical axis is also axis of symmetry. Power of Gaussian beam is centered into a narrow cone. Gaussian beam profile is shown on Fig. 2. Radius of Gaussian beam $w(z)$ can be calculated using the equation [2], [3], [9]

$$w(z) = w_0 \sqrt{1 + \left(\frac{z}{z_0}\right)^2}\,, \tag{1}$$

where w_0 is half-width at its narrowest point, z is observation plane distance, z_0 is Rayleigh distance. This distance can be described as longitudinal direction of propagation of the waist to the point, where the transverse cross-section area is doubled, z_0 can be calculated [9], [10]

$$z_0 = \frac{\pi \cdot w_0^2}{\lambda}\,, \tag{2}$$

where λ is the wavelength of radiation.

Divergence angle Θ can be calculated by this equation

$$\theta = \frac{\lambda}{\pi \cdot w_0}. \tag{3}$$

For the Gaussian curvature deals [3], [9], [10]

$$R(z) = z\left[1+\left(\frac{z_0}{z}\right)^2\right]. \tag{4}$$

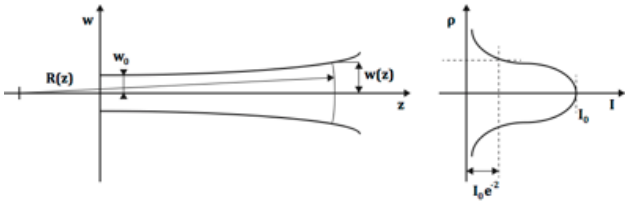

Fig. 2: Gaussian beam profile [2], [3], [4].

2.1. Optical Intensity of Gaussian Beam

Intensity of an optical radiation is a function of axial distance z (going in the direction of axis) and radial distance ρ (going in the direction of radius). Radial distance can be expressed as [2], [3], [4], [10]

$$\rho = \sqrt{x^2 + y^2}\ , \tag{5}$$

then intensity of Gaussian beam will be

$$I(\rho, z) = I_0\left(\frac{w_0}{w(z)}\right)^2 \cdot \exp\left(-\frac{2\rho^2}{w^2(z)}\right). \tag{6}$$

Gaussian beam intensity is greatest in the center of beam (axial distance z and radial distance ρ equals 0). Gaussian beam radius $w(z)$ is growing with increasing axial distance z. Intensity of Gaussian beam is decreasing with increasing axial distance z.

2.2. Optical Power of Gaussian Beam

The total power transmitted by beam is determined by the integral of the product of the radiation intensity and cross-sectional area of the optical beam [2], [9], [10]

$$P = \int_0^\infty I(\rho, z) \cdot 2\pi \cdot \rho \cdot dp\ , \tag{7}$$

from which we deduce

$$P = \frac{1}{2} I_0\left(\pi \cdot w_0^2\right). \tag{8}$$

The power of the Gaussian beam is given as the product of half of the maximal intensity and area of a circle with a radius equals to the radius of a central beam [2], [9], [10].

3. Transmission Media

FSO links are used for wireless data transmission in specific conditions. FSO uses atmosphere as a media for communication. This is associated with the disadvantage of using FSO. In adverse conditions it may be difficult to transfer data, sometimes it is impossible. It is influenced by seasons and actual weather. Most connections are built in areas between buildings; it is always in troposphere layer. Troposphere reaches a height about 10 kilometers above the sea level [19].

Refractive index is one of the basic variables describing the propagation of light in materials. It applies directly to given environment. A number of changes occurring in the atmospheric transmission environment changes refractive index. Local temperature and pressure changes have an effect on refractive index, so that is random function of time and space. Optical beam passing through these changes is influenced and this leads to change its local shape and power of the beam. The main effects influencing transmission of optical signals include [2], [3], [4], [11], and [13]:

- extinction of optical intensity due to turbulence in the atmospheric environment,
- extinction due to scattering and absorption on molecules and aerosols,
- optical intensity fluctuations due to turbulence in the atmospheric environment,
- optical intensity fluctuations due to fog, rain, snow, etc.,
- short-term disruption of beam caused by flying birds.

These effects can be further divided according to the influence, which they arise (due to turbulence in the atmosphere, the effects of fog, rain and snow, scattering and absorption on molecules). These effects influence each other and always act together. Fluctuations in optical intensity also cause extinction [9], [10].

Mean extinction coefficient on molecules can be calculated as the sum of extinction coefficients [10],

$$\alpha_e = \alpha_{abs} + \alpha_{s,m} + \alpha_{s,p} + \alpha_{fluct}\ , \tag{9}$$

where α_{abs} is coefficient of scattering on molecules, $\alpha_{s,m}$ is the coefficient of scattering – Rayleigh scattering, $\alpha_{s,p}$ is the coefficient of scattering - Mie scattering and α_{fluct} is coefficient of decreasing due to fluctuations.

3.1. Attenuation by Beam Transmission

This attenuation is important parameter, which has greatest effect on the transferred power through atmospheric media. This attenuation can be calculated by

this formula:

$$\alpha_{12} = \left| 20 \cdot \log \frac{L_0}{L_0 + L_{VP}} \right|, \quad (10)$$

where L_{VP} is a distance between optical head, L_0 is assistant length. This L_0 can be calculated from diameter of optical transmission system D_{VOS} and the angular width of the transmitted beam φ_{VS}:

$$L_0 \approx \frac{D_{VOS}}{\varphi_{VS}}, \quad (11)$$

Substituting into the equation of α_{12} (10) we get more practical formula for attenuation by beam transmission:

$$\alpha_{12} = \left| 20 \cdot \log \frac{D_{VOS}}{\varphi_{VS} + L_{VP}} \right|. \quad (12)$$

1) Rayleigh Scattering

Scattering can dramatically affect the transfer in atmospheric media. Scattering is not energy loss directly, but rather a change of direction or redistribution of light.

Rayleigh scattering is on molecules of gas or other particles that are smaller than wavelength. It is spectrally dependent on wavelength. Rayleigh scattering is omnidirectional [9], [10].

Rayleigh scattering can be calculated

$$I_\theta = I_0 \cdot \frac{\pi^2 \cdot \alpha^2}{2 \cdot \varepsilon_0^2 \cdot \lambda^4} \cdot \frac{F(\theta)}{r^2}, \quad (13)$$

where I_Θ is the intensity of light scattered by one particle Θ, I_0 is total intensity of incident radiation, ε_0 permittivity of vacuum ($8{,}85419 \cdot 10^{-12}$ $C^2 \cdot J^{-1} \cdot m^{-1}$), λ wavelength, r distance of the intensity detector, Θ view angle, $F(\Theta)$ in a function of viewing angle and α polarization from Clausius-Mossotti equation.

This parameter can be calculated using following formula [9], [10]:

$$\alpha = 3 \cdot \varepsilon_0 \cdot v \cdot \frac{n_1^2 - n_0^2}{n_1^2 - 2n_0^2}, \quad (14)$$

where we count with indexes of dispersion environment refraction n_1, clear environment refraction n_0 and permittivity of vacuum ε_0 ($8{,}85419 \cdot 10^{-12}$ $C^2 \cdot J^{-1} \cdot m^{-1}$).

2) Mie Scattering

Mie scattering occurs when the light hits the particle (drop of water, snow, etc.) as large or larger than the wavelength. It is highly variable component of extinction, because the atmosphere is changing very often. This effect is spectrally independent, that means that is not dependent on the wavelength. Mie scattering is directional effect [9], [10].

3.2. Turbulence

Atmospheric turbulences affecting beam transmission through the media can be divided into three groups:

- dynamic turbulence,
- thermal turbulence,
- mechanical turbulence.

Dynamic turbulence arise in areas about 5-6 km and do not affect free space optics links. Thermal and mechanical turbulence occurs at low altitudes and affecting FSO links [5], [6], [7].

During the day, when the Earth surface is warmer than the ambient air, the air layer closer to the surface is also warmer. This causes the rising of warm air masses upward, but also diffraction of the optical beam upward. If this rising is sufficiently large, it may result in an effect known as “mirage” (mirroring). The situation is reversed at night and optical beam is bending downwards. Besides these effects, the atmospheric turbulences disturb also the coherence of the propagated beam. Beam distortion caused by turbulence results in a divergence beam, changing the position of the beam center resulting to fluctuations and scintillations [5], [6], [7], [8], [14].

Due to temperature changes and wind speed variations forms local unstable air masses, which are divided into turbulent air bubbles with different sizes [9].

To calculate the attenuation caused by the turbulence we use the following formula based on Rytov approximation [12]:

$$\alpha_{turb} = 2 \cdot \sqrt{23{,}17 \cdot k^{7/6} \cdot C_n^2 \cdot L^{11/6}}, \quad (15)$$

where k represents the wave number, which is dependent on wavelength, C_n^2 is a structural parameter of the refractive index and L is the distance between optical heads. The resulting value α_{turb} represents the mean value of attenuation caused by turbulence [7], [8], [11].

Structural parameter of refractive index used in formulas to calculate the attenuation is a measure for determining the strength of turbulence. The value of this parameter ranges from 10^{-14} $m^{2/3}$ to 10^{-12} $m^{2/3}$ depending on strength of the turbulence, as seen in Tab. 1.

Atmospheric turbulence is affecting FSO links with these effects [14]:

- fluctuations caused by incidence of the angle of the optical beam,
- scintillation - optical intensity fluctuations,
- divergence of the optical beam,
- changes of position of optical beam center.

Tab.1: Effect of turbulence on structural parameter of refractive index.

Structural parameter of refractive index C_n^2 [$m^{-2/3}$]	Strength of turbulence
10^{-14}	Weak
10^{-13}	Medium
10^{-12}	Strong

4. Realized FSO Link

Realized link was created using professional MRV optical heads TS5000G (Fig. 3). The distance (Fig. 4) between connected points is 1,47 kilometers and divergence is 2 mrad, so we can calculate the beam width with simple goniometric function. The beam width on the receiver side is 2,94 m.

Tab.2: MRV TS5000G specification.

Model	TS5000G
Power Supply	230V AC
Capacity	1x 1,25 Gbit·s^{-1}
Laser Power	2x 40 mW, 1x 60 mW
Wavelength	830–860 nm
Beam divergence	2 mrad
Field of view RX	5 mrad
Sensitivity	-33 dBm
Eye safety Class	1M
Azimuth	107,26 °
Elevation	-0,47 °
Interface	1000Base-LX Gigabit Eth.

Fig. 3: Applied FSO head MRV TS5000G.

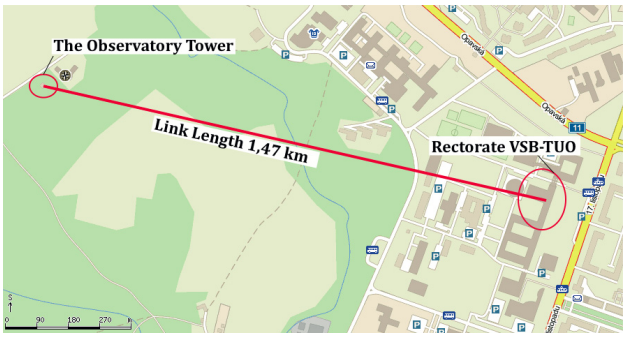

Fig. 4: Map with points of realized FSO link.

5. Measuring Device

To be able to measure the optical beam cross-section it was necessary to construct a measuring device (Fig. 5). The base of the measuring device has been borrowed from University of Technology in Brno. It is a device manufactured by Festo for movement in axes with stepper motors.

First, it was necessary to connect the basic parts of device. Then it was needed to connect device with a computer. This was done with two crossed serial RS-232 cables, one for each axis.

Then it was using application Festo Configuration Tool (FCT) to set the basic parameters such as type of axis, axis length, motor type, setting the limit sensors, etc. With this application you can also test the functionality and correct behavior of the whole equipment. With possibilities of FCT it was not possible to measure the optical beam cross section, so it was necessary to write the whole new application. It includes motion axes control, but also taking values from optical power meter.

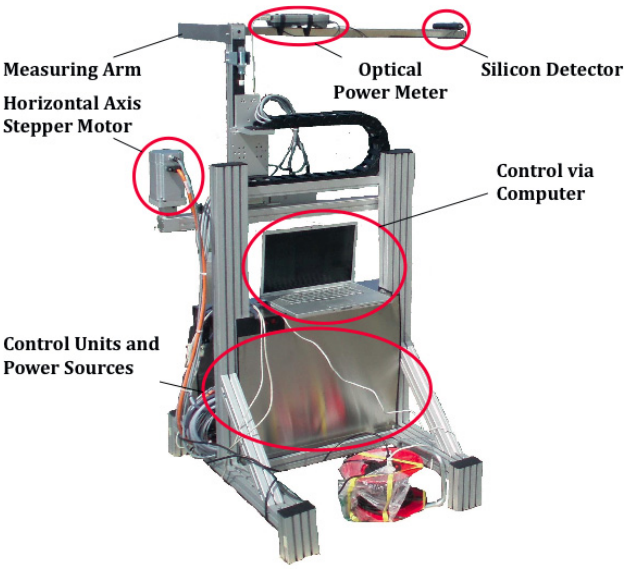

Fig. 5: Measuring device [20].

5.1. PC Application for Measurement

This application was created in an environment of MATLAB R2009a (Fig. 6). In this application, you can set all parameters that are important for proper measurement. These parameters include the selection of COM ports, the measured wavelength, the required step on axis and time to stabilize the measuring arm [20].

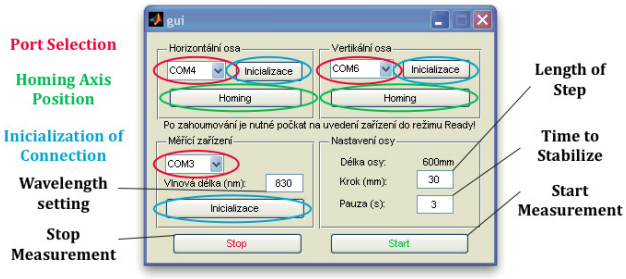

Fig. 6: Graphic user interface of measuring application.

5.2. Measurement Method

When you start measuring, power meter will pass through the grid (Fig. 7) from the starting position on horizontal axis. Once power meter arrives at the end of the axis, it comes back to the beginning of the horizontal axis and moves vertical axis one step down. Then again passes through all points of the horizontal axis, as shown in Fig. 7. At each stop removes the value from the power meter and stores it into the matrix. The resulting matrix is rendered into 3D graph and displayed to the user.

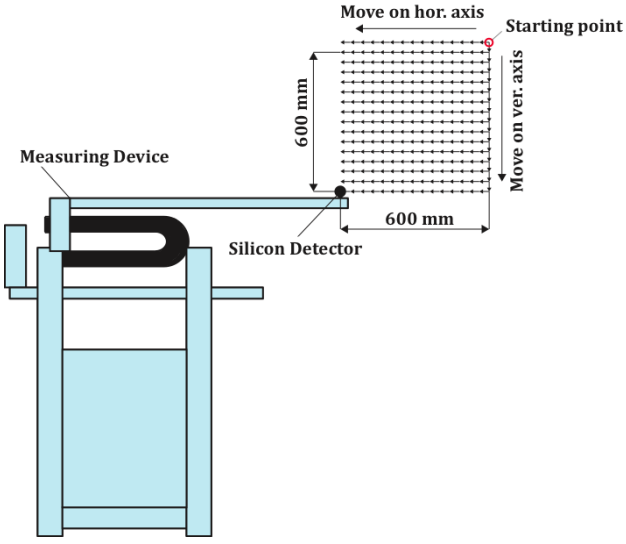

Fig. 7: An example of measurement grid with 40 mm step [20].

5.3. Measurement During Daylight

At the first measurements it was found that the ambient sunlight greatly influences the measurement, even if the power meter detector was overshadowed against direct sunlight with black tube. Several measurements were done at wavelengths 830-860 nm with different steps, but the measurement has always been very influenced by parasitic light. The taken values of optical power during the day with a clear sky were between 40-60 μW. The values taken at night were about 1 μW. So values taken in daylight were unusable and did not testify about the shape of the measured beam. For measurement was used power meter Thorlabs PM 120 and silicon detector S120B with measurement range from 50 nW to 50 mW, operating at λ between 400 nm and 1100 nm.

5.4. Measurement on April 21 During Night

Graph in Fig. 8 was measured on April 21, 2011 in following conditions: temperature 18,7 °C, humidity 44 %, no wind, pressure 1015,6 hPa. This graph was measured using two measurements when the equipment was moved after first measurement and resulting values were combined. Thereby was reached axis size 1200 mm. You can see a large optical power in the areas around the center location of the optical head (right side of the graph) and decreasing power values away from head. In all measurements it was used all 3 transmitting lasers (2x 40 mW, 1x 60 mW). For small distances (less than 300 m) it is possible to turn some lasers off.

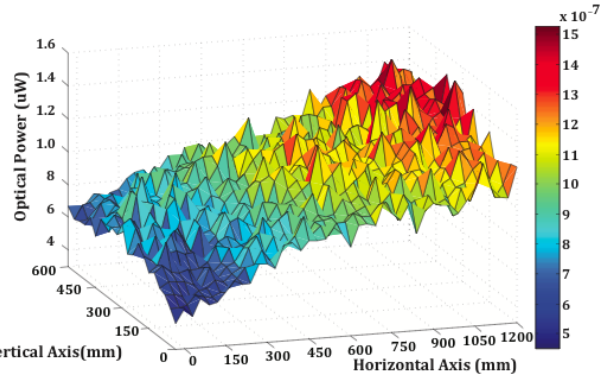

Fig. 8: Optical power measured on April 21, 2011 at 21:00 [20].

5.5. Measurement on April 25 During Night

Graph in Fig. 9 was measured on April 25, 2011 in following conditions: temperature 11,7 °C, humidity 77 %, southeast wind 0,03 m/s, pressure 1017,8 hPa. Graph was measured by three independent measurements and then values were properly combined. This allowed capturing a larger beam width (3x 600 = 1800 mm), on which we can see the top of the beam with high optical power and sloping edge of the beam on both sides. In this measurement was taken approximately 61 % of beam width. On the graph we can observe many peaks, which are caused by measuring time, which is about 30 minutes and also by changing atmospheric media.

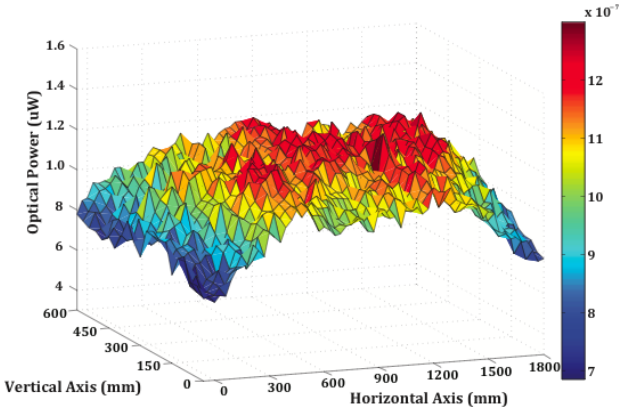

Fig. 9: Optical power measured on April 25, 2011 at 21:00 [20].

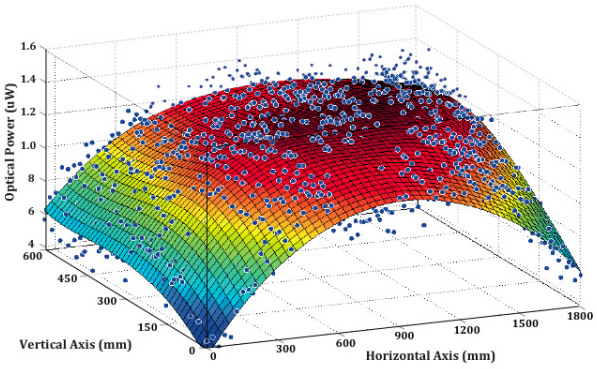

Fig. 10: Smoothed optical power of beam measured on April 25, 2011 at 21:00 [20].

5.6. LOWESS Smoothing of Measured Graph

Graph in Fig. 9 is still influenced by the effects of atmospheric environment, so it was suitable to smooth this graph, as you can see in Fig. 10. Graph was interspersed in MATLAB R2009a with quadratic polynomial function LOWESS (Locally Weighted Scatterplot Smoothing), to highlight a shape of optical beam. This function uses locally weighted regression proposed by Cleveland in 1979 [15].

The following is a sketch of the LOWESS algorithm [16], [17], [18]:

- count the number of points in the neighborhood. This is number of points times LOWESS fraction rounded to the nearest integer. This number is called q,
- use tricube function to generate a weighted least squares fit. The weight given to point (x_k, y_k) is:

$$w_k = T\cdot\left(\frac{x_i - x_k}{d_i}\right)$$
$$T(u) = \begin{cases}\left(1-|u|^3\right)^3 & for\ |u|<1\\ 0 & otherwise\end{cases}, \quad (19)$$

where d_i is distance from x_i to its q^{th} nearest neighbor, T is tri-cube weight function [15], [16].

- Compute the residuals of this fit.
- Compute a bi-square weight function of the residuals.
- Use the horizontal weight multiplied by the vertical weights in a weighted least squares fit.

Smoothing was calculated with a range of 50 %, when the R-Square value was 0,7948. The R-Square is a parameter indicates how close the regression to real data values is. When the R-Square value is 1, model is consistent with the data.

5.7. Smoothing with Gaussian Function

For smoothing graph of optical power was also used Gaussian function (Fig. 11). This function should better correspond with the real beam, because the original signal should be Gaussian-shaped beam. For smoothing was used this function:

$$f(x,y) = A\cdot e^{-\left[\frac{(x-x_0)^2}{2\cdot\sigma_x^2}+\frac{(y-y_0)^2}{2\cdot\sigma_y^2}\right]}. \quad (20)$$

Tab.3: Coefficients (with 95 % confidence bounds).

A	$11{,}86\cdot10^7$ (11,79; 11,93)
σ_X	24,58 (22,99; 26,18)
σ_Y	45,69 (44,51; 46,86)
$\mathbf{X_0}$	11,88 (11,45; 12,3)
$\mathbf{Y_0}$	25,00 (24,5; 25,5)

Sum of Squares Due to Error (SSE) is a parameter measures the total deviation of the response from the fit to the response values.

Root Mean Squared Error (RMSE) - this statistic is also known as the fit standard error and the standard error of the regression. It is an estimate of the standard deviation of the random component in the data.

Tab.4: Goodness of fit.

SSE	606
R-square	24,58 (22,99; 26,18)
Adjusted R-square	45,69 (44,51; 46,86)
RMSE	11,88 (11,45; 12,3)

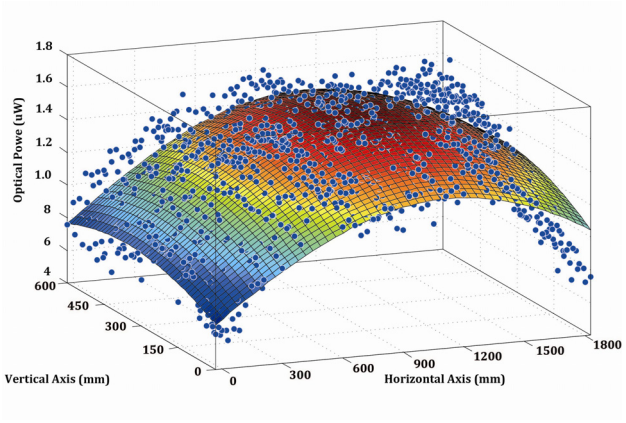

Fig. 11: Optical power of beam measured on April 25, 2011 at 21:00 smoothed with Gaussian function [20].

6. Conclusion and Future Work

This article summarizes the creation of the measuring device, including PC application. This device can measure optical power of beam cross-section with desired accuracy. The disadvantage of this device may be relatively small measuring area, which is particularly true for connections with large distances, where because of the influence of beam divergence does not measure the whole shape of optical beam. In this time it is ordered horizontal axis of length 2 meters solving this problem for future work.

This will allow larger scale of measuring device without having to push or other manipulations during measurement. It is also planned to automation of equipment to measure the statistics of optical beam in various weather conditions. This will include automating of steps necessary for measurements with built-in PC, operated via remote control using VNC software application. The measurements will be repeated in time periods (e.g. every day) and the results will be statistically processed.

Consideration is also creation of a completely new program in the LabVIEW environment that would better satisfy requirements for reliability and ease of modifiability of the program for measuring. One of the essential objectives is to ensure protection of equipment against weather conditions, which will include the creation of such covers and seal, to avoid any intrusion of water and other particles into the device.

Acknowledgements

I would like to thank to prof. Otakar Wilfert, Jan Diblik for rental a base for measuring device. This article was supported by project GACR (Czech Science Foundation) GA102/09/0550 – Study of optical beams for atmospheric static and mobile communications. This work was supported also by the Ministry of Education of the Czech Republic within the projects no. SP2011/47, SP2011/180 of the VSB - Technical University of Ostrava.

References

[1] CÍSAŘ, D. *Vliv atmosférických turbulencí na intenzitní profil laserového svazku*. Brno, 2009. p. 42. Bachelor Thesis. Brno University of Technology, The Faculty of Electrical Engineering and Communication.

[2] GBUR, G.; WOLF, E. Spreading of partially coherent beams in random media. *Journal of the Optical Society of America A: Optics and Image Science, and Vision*, 2003, Vol. 19, No. 8, pp. 1592-1598. ISSN 1084-7529.

[3] SHIRAI, T.; DOGARIU, A.; WOLF, E. Directionality of some model beams propagating in atmospheric turbulence. *Optics Letters*, 2003, Vol. 28, No. 8, pp. 610-612. ISSN 0146-9592.

[4] RICKLIN, J., C.; DAVIDSON, F., M. Atmospheric optical communication with a Gaussian Schell beam. *Journal of the Optical Society of America A: Optics and Image Science, and Vision*, 2003, Vol. 20, No 5, pp. 856-866. ISSN 1084-7529.

[5] KON, A., I.; TATARSKII, V., I. On the theory of the propagation of partially coherent light beams in a turbulent atmosphere. *Radiophysics and Quantum Electronics*, 1974, Vol. 15, No. 10, pp. 1187-1192. ISSN 0033-8443.

[6] WANG, S., C., H.; PLONUS, M., A. Optical beam propagation for a partially coherent source in the turbulent atmosphere. *Journal of the Optical Society of America*, 1979, Vol. 69, No. 9, pp. 1297-1304. ISSN 0030-3941.

[7] KOROTKOVA, O.; ANDREWS, L.; C., PHILLIPS, R. L. Model for a partially coherent Gaussian beam in atmospheric turbulence with application in lasercom. *Optical Engineering*, 2004, Vol. 43, No. 2, pp. 330-341. ISSN 0091-3286.

[8] RICKLIN, J., C.; DAVIDSON, F., M. Atmospheric turbulence effects on a partially coherent Gaussian beam: Implications for free-space laser communication. *Journal of the Optical Society of America A: Optics and Image Science, and Vision*, 2002, Vol. 19, No 9, pp. 1794-1802. ISSN 1084-7529.

[9] HENNIGER, H.; WILFERT, O. An Introduction to Free-space Optical Communications. *Radioengineering*. 2011, Vol. 19, No. 2, pp. 203-212. ISSN 1210-2512.

[10] ANDREWS, L., C. Field Guide to Atmospheric Optics. In: *SPIE Publications - The International Society for Optical Engineering*, 2004, pp. 112, ISBN 978-0819453181.

[11] AL NABOULSI, M.; SIZUN, H.; DE FORNEL, F. Fog attenuation prediction for optical and infrared waves. *Optical Engineering*. 2004, Vol. 43, No. 2, p. 319-329. ISSN 0091-3286.

[12] BÁRTA, M. *Vliv atmosférických turbulencí na optický svazek*. Brno, 2009. p. 92. Master thesis. Brno University of Technology, The Faculty of Electrical Engineering and Communication.

[13] ANDREWS, L., C.; PHILLIPS, R., L.; HOPEN, C., Y.; AL-HABASH, M., A. Theory of optical scintillation. *Journal of the Optical Society of America A*. 1999, Vol. 16, No. 6, p. 1417 – 1429. ISSN 0740-3232.

[14] WEISS-WRANA, K., R. Turbulence statistics in littoral area. In: *Proceedings of SPIE - The International Society for Optical Engineering*, 6364, art. no. 63640F. 2006. ISBN 978-081946459-0.

[15] BURDÍKOVÁ, M. Aplikace robustní vážené lokální regrese na teplotní časové řady. In: *Sborník ROBUST 92*. 1992, pp. 21 - 30. Available at WWW: <http://www.statspol.cz/robust/1992_budiko92.pdf>.

[16] Locally Weighted Scatterplot Smoothing (LOWESS). In MUKHERJEE, Chandan. *Thinking With Data* [online]. 2011 [cit. 2011-09-04]. Available at WWW: <http://development.thinkingwithdata.com/classnotes/lowess.pdf>.

[17] HOWARTH, R., J. A history of regression and related model-fitting in the earth sciences (1636-2000). *Natural Resources Research*. 2001, Vol. 10, No. 4, pp. 241-286. ISSN 1520-7439.

[18] LOWESS SMOOTH. In: *DATAPLOT Reference Manual* [online]. 1996 [cit. 2011-09-04]. Available at WWW: <http://itl.nist.gov/div898/software/dataplot/refman1/ch3/lowess_s.pdf>.

[19] ŠÁLA, J. *Bezdrátový optický spoj*. Brno, 2010. p. 70. Master thesis. Brno University of Technology, The Faculty of Electrical Engineering and Communication.

[20] DAVID, T. Testovací měření na profesionálním atmosférickém optickém spoji, Ostrava, 2011. p. 97. Bachelor thesis. VSB – Technical university of Ostrava, Faculty of Electrical Engineering and Computer Science.

About Authors

Tomas DAVID was born in 1989 in Valasske Mezirici. He received a B.Sc. Degree at the Technical University of Ostrava, Faculty of Electrical Engineering and Computer Science in 2011. Currently in Master degree studies he focuses on optical technologies and especially Free Space Optics links.

Jan LATAL was born in Prostejov. He received his B.Sc. Degree from the VSB-Technical University of Ostrava, Faculty of Electrical Engineering and Computer Science, Dept. of Electronic and Telecommunications in 2006. He received his M.Sc. Degree from the Technical University of Ostrava, Faculty of Electrical Engineering and Computer Science, Dept. of Telecommunications in 2008. Currently in doctor degree studies, he focuses on optical technologies (xPON) and especially on free space optics, fiber optics sensors etc. He is a member of SPIE.

Frantisek HANACEK was born in 1981 in Uherske Hradiste. In 2006 he finished M.Sc. study at VSB-Technical University of Ostrava, Faculty of Electrical Engineering and Computer Science, Deptartment of Telecommunications. In the present time during his Ph.D. study he is interested in Fiber optic sensors and Distributed Temperature Sensing systems.

Petr KOUDELKA was born in 1984 in Prostejov. In 2006, he finished bachelor study at VSB-Technical University of Ostrava, Faculty of Electrical Engineering and Computer Science, Dept. of Electronic and Telecommunications. Two years later, he finished M.Sc in the field of optoelectronics. In the present time during his Ph.D. study he is interested in Free Space Optics and Distributed Temperature Sensing systems.

Jan VITASEK was born in 1984 in Opava. In 2009 he finished M.Sc. study at Brno University of Technology, Faculty of Electrical Engineering and Communication. In present time he is Ph.D. student at VSB – Technical University of Ostrava. His interests are propagation and processing of optic signals.

Petr SISKA was born in 1979 in Kromeriz. In 2005 he finished M.Sc. study at VSB-Technical University of Ostrava, Faculty of Electrical Engineering and Computer Science, Dept. of Electronic and Telecommunications. Three years later, he finished Ph.D. study in Telecommunication technologies. Currently he is employee of Department of Telecommunications. He is interested in Optical communications, Fiber optic sensors and Distributed Temperature Sensing systems.

Jan SKAPA was born in Ostrava, Czech Republic in the year of 1980. He reached the Ph.D. in Telecommunication technologies in 2009. He's professional interests involves optical communication systems, optical fiber sensors, digital signal processing and speech and image processing.

Vladimir VASINEK was born in Ostrava. In 1980 - he graduated at the Science Faculty of the Palacky University, branch - Physics with specialization in Optoelectronics, RNDr. he obtained at the Science Faculty of the Palacky University at branch Applied Electronics, scientific degree Ph.D. he obtained in the year 1989 at branch Quantum Electronics and Optics, he became an associate professor in 1994 at branch Applied Physics, he is a professor of Electronics and Communication Science since 2007 and he works at this branch at the Department of Telecommunications of the Faculty of Electrical Engineering and Computer Science. His research work is dedicated to optical communications, optical fibers, optoelectronics, optical measurements, optical networks projecting, fiber optic sensors, MW access networks. He is a member of many societies - OSA, SPIE, EOS, Czech Photonics Society, he is a chairman of Ph.D. board at the Technical University of Ostrava, and he was a member of many boards for habilitation and professor appointment.